Available online at www.sciencedirect.com
ScienceDirect
Journal of Computational Physics 227 (2008) 2118–2129
JOURNAL OF COMPUTATIONAL PHYSICS
www.elsevier.com/locate/jcp

Symmetry reduction for molecular dynamics simulation of an imploding gas bubble

Alexander Bass [a,*], Seth Putterman [a], Barry Merriman [b], Steven J. Ruuth [c]

[a] Department of Physics and Astronomy, University of California at Los Angeles, Los Angeles, CA 90095, United States
[b] Department of Mathematics, University of California at Los Angeles, Los Angeles, CA 90095, United States
[c] Department of Mathematics, Simon Fraser University, Burnaby, British Columbia, Canada V5A 1S6

Received 4 June 2007; received in revised form 12 October 2007; accepted 18 October 2007

Abstract

We propose a symmetry reduction technique whereby molecular dynamics (MD) simulations for spherically symmetric gas bubbles can be accelerated. Results for an imploding Xenon bubble containing 50 million particles—the smallest measured sonoluminescing system—are presented.

PACS: 78.60.Mq; 02.70.Ns

Keywords: Sonoluminescence; Molecular dynamics; Imploding bubble

1. Introduction

Sonoluminescence (SL) is the phenomenon whereby the passage of sound through a fluid causes a trapped bubble to pulsate so violently that it emits flashes of light [1–5].

During the rarefaction half-cycle of the acoustic wave, the bubble expands to its maximum radius, typically an order of magnitude greater than its ambient radius. As the rarefaction gives way to compression the bubble begins to collapse. This collapse continues well beyond the ambient radius due to the high inertia of the liquid and the bubble eventually implodes with a supersonic velocity and its interior reaches temperatures and pressures inside large enough to produce a flash of light. Light emission occurs because the input acoustic energy is focused by many orders of magnitude.

There are a number of unanswered questions about sonoluminescence: the foremost of them being the detailed mechanism of transduction of sound into light. Experiments have not reached the point where parameters such as temperature and density have been measured as a function of position inside of the bubble. Furthermore, in view of the supersonic or near supersonic velocity of collapse, sharp gradients

* Corresponding author. Tel.: +1 310 825 1842; fax: +1 310 206 5668.
E-mail address: bass@physics.ucla.edu (A. Bass).

0021-9991/$ - see front matter
doi:10.1016/j.jcp.2007.10.013

in density are expected to form inside of the bubble. Hydrodynamic models [6–10], however, assume local thermodynamic equilibrium everywhere within the bubble, i.e. near constancy of macroscopic thermodynamic variables over molecular scattering lengths and collisional time scales. Though this assumption certainly holds for the greater part of the bubble's collapse it does break down near the minimum radius [11] where SL originates. Another limitation of hydrodynamic models is that they require the knowledge of the equation of state for the gas as well as transport processes for the very extreme conditions of the bubble's dynamics.

Molecular dynamics (MD) simulations [12,13] are, on the other hand, free of the above limitations as they directly apply the mechanical laws to predict the trajectory of each individual gas particle. A comprehensive MD model of SL was presented in Ref. [11]. It treated the bubble as a hard sphere gas driven by a spherical piston moving in accordance with the Rayleigh–Plesset equation and also included a simple ionization model. With this model the authors were able to simulate bubbles containing up to 10^6 particles on a single workstation-grade computer with the simulation taking a few days to complete. MD simulations of an imploding bubble have also been considered in Refs. [14–16]. The goal of this paper is to extend the capabilities of the MD method so as to be comparable in size with real-life SL systems.

2. The model

2.1. Description of the MD model

Our present work is based on the model of Ref. [11], a brief summary of which follows.

2.1.1. The bubble wall

This model focuses on the simulation of single bubble sonoluminescence, so that results can be compared to the best studied experimental SL systems. Such bubbles remain spherical during their collapse, and their behavior is parametrized by their ambient radius (the radius they have when at rest at the ambient pressure) and their maximum radius (the radius they attain when maximally expanded at the low pressure point of the applied sound field). The ambient radius, R_0, is related to the number of gas particles, N, by the ideal gas equation of state

$$P_0\left(\frac{4}{3}\pi R_0^3\right) = kT_0N, \tag{1}$$

where $T_0 = 300$ K and $P_0 = 1$ atm are the ambient temperature and the pressure. The maximum radius R_m is chosen to yield the ratio of $R_m/R_0 = 10$, as is typical in experimental SL bubbles.

Since the bubble remains spherical during collapse, its boundary dynamics are described entirely by the radius as a function of time, $R(t)$. We are concerned with energy focusing processes and gas dynamics inside the bubble, and in this spirit we will take $R(t)$ as being known. A convenient model of the spherical piston that captures some qualitative features of the supersonic collapse is provided by Rayleigh–Plesset equation [2]

$$R\ddot{R} + \frac{3}{2}\dot{R}^2 = [P_g(R) - P_0]/\rho \tag{2}$$

with a van der Waals hard core equation of state

$$P_g(R) = \frac{P_0R_0^{3\gamma}}{(R^3 - a^3)^\gamma}, \tag{3}$$

$\gamma = 5/3$, where a is the radius of the gas in the bubble when compressed to its van der Waals hard core ($R_0/a = 7.84$ for Xe), ρ is the density of the surrounding fluid, and the initial condition for the solution to Eq. (2) is that $\dot{R} = 0$ when $R = R_m$.

We emphasize that the derivation of Eqs. (2) and (3) applies only for small Mach number motion and thus they are invalid as a fundamental theory for SL [1]. Eq. (2) also neglects viscous damping, acoustic radiation and surface tension. However, it still reasonably approximates the gross bubble pulsation, which justifies its use in our initial study.

2.1.2. Gas dynamics

It has been observed that for SL in water, the bubble must contain sufficient amount of a noble gas. Thus in many single bubble SL experiments, the water is first degassed to remove atmospheric gases, and then re-saturated with a noble gas to produce pure noble gas bubbles. We will focus our gas dynamic model on this system, since it is a frequent experimental model and also because it allows the simplest molecular gas dynamics models. Because the gas is noble, it consists of isolated atoms that do not engage in chemical reactions. Thus we can model it with simple gas particles that have no rotational or internal vibrational degrees of freedom, and which do not engage in any chemical reactions with the water walls of the bubble, even at elevated temperatures.

Molecular dynamics simulations for such simple gas particles fall into two broad categories, defined by the way they treat interatomic forces. The forces can either be given by a potential that varies continuously with radius from the atom center (''soft sphere''), or by a potential that is a step function of radius (''hard sphere''). The latter particles behave simply like billiard balls. While the continuous potential are more physically realistic, they are also much more costly to compute with. For that reason we choose the *hard sphere* model.

A hard sphere system evolves in time by a series of discrete collision events. No explicit numerical integration is needed since impulsive collisions are carried out only when atoms interact, and between collisions each atom follows an independent linear trajectory. To illustrate, consider two particles separated by a relative position $\mathbf{r}$ and having a relative velocity $\mathbf{v}$. These particles collide if their separation equals the atomic diameter σ at some time t in the future. If such a collision occurs, then t is the smaller positive solution of

$$|\mathbf{r} + \mathbf{v}t| = \sigma, \tag{4}$$

which has a solution

$$\tau = -\frac{1}{\mathbf{v}\cdot\mathbf{v}}\left[\mathbf{r}\cdot\mathbf{v} + \sqrt{(\mathbf{r}\cdot\mathbf{v})^2 - (\mathbf{v}\cdot\mathbf{v})(\mathbf{r}\cdot\mathbf{r} - \sigma^2)}\right] \tag{5}$$

Collisions are carried out impulsively so that the change in velocities preserves energy and momentum. Specifically,

$$\Delta\mathbf{v}_1 = -\Delta\mathbf{v}_2 = -\frac{(\mathbf{r}_c\cdot\mathbf{v})\mathbf{r}_c}{\sigma^2}, \tag{6}$$

where $\Delta\mathbf{v}_1$ is the change in velocity of the first particle, $\Delta\mathbf{v}_2$ is the change in velocity of the second particle and $\mathbf{r}_c$ is the relative position at the time of collision.

2.1.3. Bubble wall boundary condition

In our present model we will exclusively use the *heat bath* boundary condition. When a particle hits the boundary it is assigned a thermal velocity, corresponding to the ambient liquid temperature T_0, in the wall's local frame of reference. Temperature T_0 is assumed constant throughout the collapse. Though an approximation, it appears to be justified on the basis that the heat capacity of the liquid is much greater than that of the gas.

2.1.4. Hard sphere properties

The basic properties associated with the hard sphere model are the gas particle mass and diameter. The mass is simply taken to be the mass of the noble gas atom being simulated. The choice of a proper hard sphere diameter is a much more difficult question. The diameter should represent the statistical average distance of approach of the particles during collisions, and thus in general it should depend on the collision energy.

A variety of models have been proposed to take this effect into account [18]. In the present work we will use the formula for the atomic diameter as a function of the collision energy provided by the variable soft sphere (VSS) model [19,20]

$$\sigma = \left(\frac{5(\alpha+1)(\alpha+2)(m/\pi)^{1/2}(kT_{\mathrm{ref}})^{\omega}}{16\alpha\Gamma(9/2-\omega)\mu_{\mathrm{ref}}E_t^{\omega-1/2}}\right)^{1/2}, \tag{7}$$

where k is the Boltzmann's constant, m is the mass of the particle, ω is the dimensionless viscosity index and α is a dimensionless constant for each gas. The constant μ_{ref} represents the viscosity at the reference temperature ($T_{\mathrm{ref}} = 273$ K) and pressure (1 atm). Finally, $E_t = (1/2)m_r c_r^2$ is the asymptotic kinetic energy, where m_r is the reduced mass and c_r is the relative velocity between the particles. For Xenon, $\omega = 0.85$, $\mu_{\mathrm{ref}} = 2.107 \times 10^{-5}\ \mathrm{N\,s\,m^{-2}}$ and $\alpha = 1.44$.

2.1.5. Ionization effects

Near the minimum radius of the bubble, collisions become sufficiently energetic to ionize the gas atoms. Ionization exerts a very strong cooling effect on the gas, since on the order of 10 eV of thermal energy is removed from the gas by each ionization event. The ions and free electrons produced by ionization will move according to Coulomb forces, but their inclusion is very expensive computationally due to the long range effects, so they will not be included in this first treatment. Instead, we will limit ourselves to the simplest possible model of ionization and will only consider the impact of ionization on energy accounting.

For the purpose of energy accounting, an ionization ultimately produces two losses: the energy of ionization is lost immediately, and the emitted cold electron will quickly be heated to thermal equilibrium with the gas through subsequent electron–gas collisions, thus extracting an additional one particle's worth of thermal energy by the equipartition of energy.

For our model, whenever the collision energy (the kinetic energy in the center of mass frame) exceeds the ionization potential we will simply assume that ionization occurs with a probability of 1 and we will deduct a suitable amount of energy from the pair. We also keep track of how many electrons each particle has lost, so that we can make use of the appropriate next ionization energies and calculate the local ionization levels. The direction of gas particle propagation is updated exactly as without ionization.

2.2. Scaling

To assess the feasibility of modeling large bubbles with MD one needs to understand how the overall simulation time scales with the number of particles in the bubble. In Ref. [11] the motion of the bubble's wall is approximated by the free collapse, no-dissipation Rayleigh–Plesset Eq. (2). For the greater part of the collapse, however, the gas pressure $P_{\mathrm{g}}(R)$ can clearly be neglected. The resulting equation,

$$R\ddot{R} + \frac{3}{2}\dot{R}^2 + P_0/\rho = 0, \tag{8}$$

is invariant under simultaneous multiplication of the radius and time by the same constant. Therefore the collapse time is approximately proportional to $R_{\max} \propto N^{1/3}$, N being the total number of particles. Using the fast cell-based algorithm of Ref. [12] the computational time is in turn proportional, for a given time of collapse and assuming similar conditions inside the bubble, to $N \log N$, where the logarithmic factor accounts for the corresponding increase in the size of the event calendar. We thus arrive at the conclusion that the computer time needed to simulate a bubble consisting of N particles goes roughly as $N^{4/3} \log N$.

One can see therefore that despite the seemingly small gap between the numbers achieved in Ref. [11] and real physical sonoluminescing systems the brute force approach would take about a year to simulate even the smallest such system known [17], containing 50×10^6 atoms.

2.3. Searching for symmetry reduction

Instead of a brute force approach we seek to take advantage of the spherical symmetry of the problem. After all, hydrodynamic simulations of a spherically symmetric system are essentially one-dimensional, and though MD can hardly be made one-dimensional, one should be able to achieve some reduction in the size of the simulated region. The following simple thought experiment will justify our approach.

Molecular dynamics simulations are designed to be completely insensitive to the *microscopic* initial conditions as long as the initial *macroscopic* state has the correct energy, momentum, etc. (In fact it is common to initialize an MD system by placing atoms in nodes of some regular structure and assigning all particles the same speed as one expects the system to thermalize very rapidly.)

Thus we imagine an SL bubble in an initial microscopic state such that its southern hemisphere is a mirror image of its northern hemisphere. In exact arithmetic, this initial symmetry will be preserved throughout the collapse. Whenever a particle from the northern hemisphere approaches the equator plane from above its mirror image approaches from below and the ensuing collision is as if both particles bounced off a rigid wall separating the two hemispheres. Thus the full system is completely equivalent to a hemispherical system, bounded by a rigid adiabatic wall.

Of course, one may continue this process of dividing the simulation region in two, resulting in quarters, octants, etc. An octant is especially easy to work with, so we choose it as our first test of this idea. All simulations presented in this paper are based on the model of Ref. [11]. We choose Xenon as the gas inside, for reasons explained below, using variable soft sphere (VSS) model for the diameter of particles, *heat bath* boundary conditions at the wall and the simple ionization model described in Ref. [11].

Fig. 1 compares the results of an octant simulation with the corresponding full sphere simulation for a Xenon bubble containing one million particles. Two snapshots are taken at the minimum radius and at the peak temperature, which occurs slightly later. As one can see from the figure the octant is virtually identical to the full sphere with the exception of statistical fluctuations in regions where density is very low.

2.4. Replacing full sphere with cone

The question now arises as to how far one can go along the path of dividing the sphere into successively smaller pieces (wedges). At the first glance it seems that it can be done indefinitely since in a spherically symmetric bubble any two wedges of the same size have to be thermodynamically equivalent to each other. On the microscopic level however the sharp corner of the wedge creates a problem. No molecule can come closer to the center of the bubble than $d/(2\sin\theta)$, where d is the diameter of the molecule and θ is the half-angle of the wedge, effectively creating vacuum in the center. Alternatively one can impose a somewhat different boundary condition, allowing the centers of particles to approach the wedge boundary rather than their edges. This would help to avoid the problem with the vacuum in the center but in effect would add extra, unphysical, volume to the simulation region. Regardless of the approach one adopts, it is clear that the small central region, on the order of $d/(2\sin\theta)$ in radius, is not treated correctly and if the wedge angle is made too small the reduced simulation will cease to resemble the actual full-sphere bubble. Xenon atoms have the largest diameter

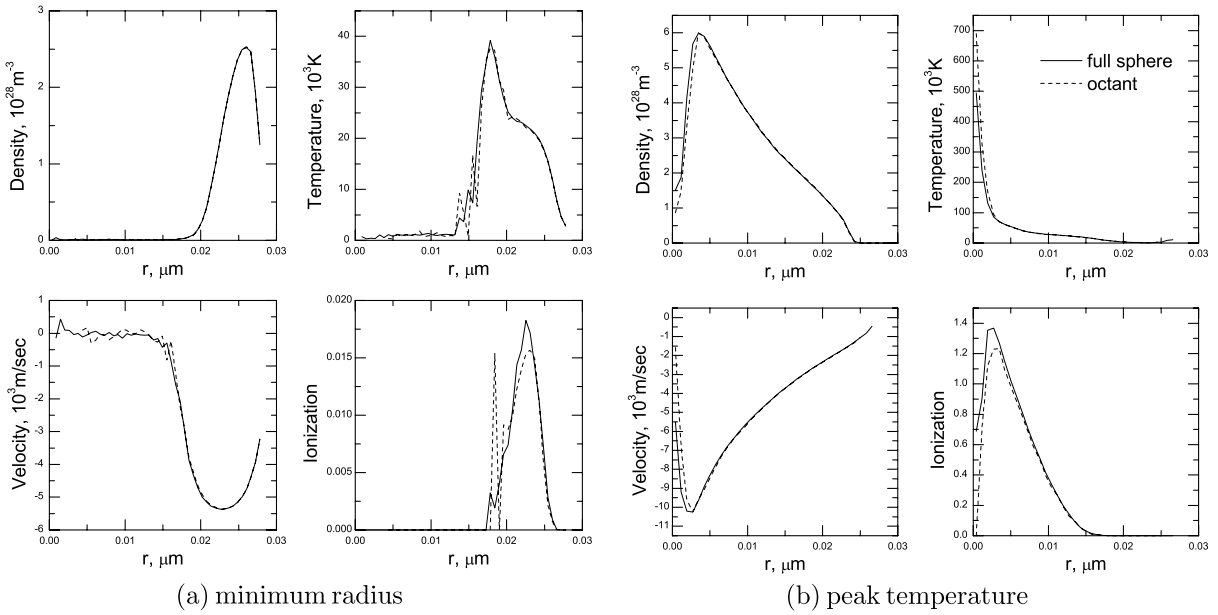

Fig. 1. Comparison of simulations of a full sphere with the corresponding octant (a) at the minimum radius and (b) at the peak temperature for a Xenon bubble containing 10^6 atoms with heat bath boundary conditions and VSS diameter particles.

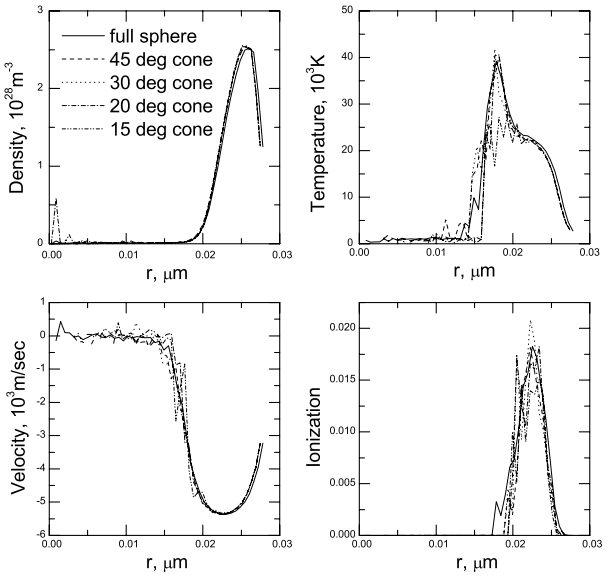

Fig. 2. Various size cones compared to the full sphere for a bubble of 10^6 Xenon atoms. Snapshots are taken at the minimum radius.

of the gases modeled in Ref. [11] making it the worst case scenario for symmetry reduced MD simulations—a reason we chose it as our test model.

Though we provided a simple theoretical justification for cutting the bubble in halves it seems unlikely that powers of 1/2 fractions of the sphere would have a special role. On the contrary, the only limiting factor seems to be the sharp angle at the center. However if we want to achieve the smallest size of the simulation region possible for a given angle the wedge shape is clearly not optimal and one is naturally led to replace it with a *cone*.

Before the cone method can be applied to modeling large bubbles we need to test it on a system small enough so that we can compare the cone against the full sphere. For the full sphere system we once again choose a Xenon bubble containing one million particles, which was the largest system modeled in Ref. [11]. We have found that the cone method produces satisfactory outcomes down to angles of about 15°, corresponding to about 17,000 particles in the cone. Fig. 2 provides, as an example, snapshots of the system taken at the minimum radius for simulations of various cone sizes. At small angles the statistical noise for temperature becomes noticeable. The reason for this is that during the final stages of the collapse the temperature peak rides ahead of the density and thus occurs in a low density region with few particles. However even in the 15° simulations, which incidentally require only about 20 min to run compared to more than a day for the full sphere, we do not yet observe significant systematic errors. This demonstrates that the cone method can be strongly beneficial for modeling large size bubbles.

3. 50,000,000 particle bubble

In this section we simulate the collapse of a sonoluminescing bubble with an ambient radius of 0.79 μm and containing a total of 50×10^6 Xenon atoms. Heat bath boundary conditions and the VSS diameter model are applied. The simulations start at the maximum radius (7.9 μm) and continue past the minimum (0.10 μm) to include the shock wave focusing, hot spot and beyond. We also analyze the convergence of the cone method and discuss its applicability.

3.1. Simulation results

As we have already mentioned, performing a full sphere simulation of systems containing more than a few million particles does not seem feasible. By using the cone it is always possible to reduce the system to any

desirable size. However it is difficult to predict *a priori* what cone angle will be sufficient for the cone simulation to represent a reasonable approximation to the full sphere. In practice one has to choose an initial angle based on the estimated run time and then compare the results with those obtained using larger and/or smaller angles.

We first present the results of the 20°, 15° and 10° simulations. They span a factor of 4 range in terms of the number of particles and are found to be in excellent agreement among themselves.

For the greater part of the collapse the conditions inside the bubble are largely uniform. As the bubble approaches its minimum radius,[1] however, we observe a dramatic increase in the density near the edge. Shortly before the minimum radius, this leads to a steeply profiled wave being launched from the boundary inward (see Fig. 3(a)). As the wave moves toward the center the temperature increases very rapidly, with the temperature peak leading the density. Eventually the temperature becomes high enough that ionization begins. This ionization subsequently leads to the cooling of the gas behind the wavefront. As the wave approaches the center the density profile essentially becomes discontinuous (see Fig. 3(b)). When this shock wave hits the center the energy focusing is so strong that the temperature[2] in the center exceeds 2×10^6 K and the gas is very strongly ionized (see Fig. 3(c)). Following this implosion the wave is reflected from the center as illustrated in Fig. 3(d).

Fig. 4 shows the temporal characteristics of the bubble collapse near the minimum radius. The temperature graph shows a very strong and sharp spike exceeding two million degrees and a peak width of no more than 0.2 ps. The peak width is an important quantity that allows us to estimate the duration of the light emission. Assuming that the emission mechanism is thermal in nature, the flash width equals the temperature peak width at the appropriate turn-on threshold level. A distinctive feature of the present simulation that can be seen in Fig. 4 is that the density and temperature peaks coincide, unlike the earlier simulation with $N = 10^6$ particles, where density lags behind the temperature. Physically this should result in a higher intensity for the light emission.

3.2. Error analysis

The errors produced by the cone simulations fall into two categories—statistical and systematic. The former appear in regions of low density where the number of particles is too small for accurate measurement of thermodynamic parameters. If desired, this type of error can be alleviated by averaging over several runs, as Fig. 5(a) demonstrates. Systematic errors, on the other hand, are artifacts of replacing the full sphere with a small part of it—the cone. From the analysis of the previous section we expect them to be especially pronounced in the central region, approximately $d/\sin\theta$ in size. Fig. 5(b) shows that the deviations observed in the bubble center around the shock focusing time are of the systematic type in the 5° simulations. To investigate this effect in more detail we plot the density, temperature, velocity and ionization at the bubble center as functions of time for various size cone simulations.

Fig. 4 shows that the main effects of reducing the size of the cone are higher densities and lower temperatures in the center as well as an overall time delay in the progression of the bubble dynamics. The figure shows that the 20°, 15° and 10° simulations are in good agreement among themselves while the 5° cone shows a significant discrepancy in temperatures, densities and timing.

In order to study the convergence of the cone method we plotted (Fig. 6) the maximum temperature and the time delay (“time at peak temperature” − “time at minimum radius”) vs. the cone angle. Both graphs display saturation toward larger angles so we fit them to an exponential decay function. This seems to approximate the data very well. Both exponentials have a characteristic “decay angle” of about 5° (“x_0” in the figure) and saturate at values (“y_0” in the figure) only marginally different from those obtained with the 20° simulation. The latter parameter gives us an estimate of what we would obtain using the full sphere simulation had we actually been able to do it.

[1] The moment we refer to as ‘the minimum radius’ is the one predicted by the Rayleigh–Plesset equation. In the actual simulation however vacuum forms near the boundary and the bubble essentially continues its collapse beyond this point.

[2] All thermodynamic quantities are obtained through averaging over spherical shells that are (1/50)th of the bubble radius.

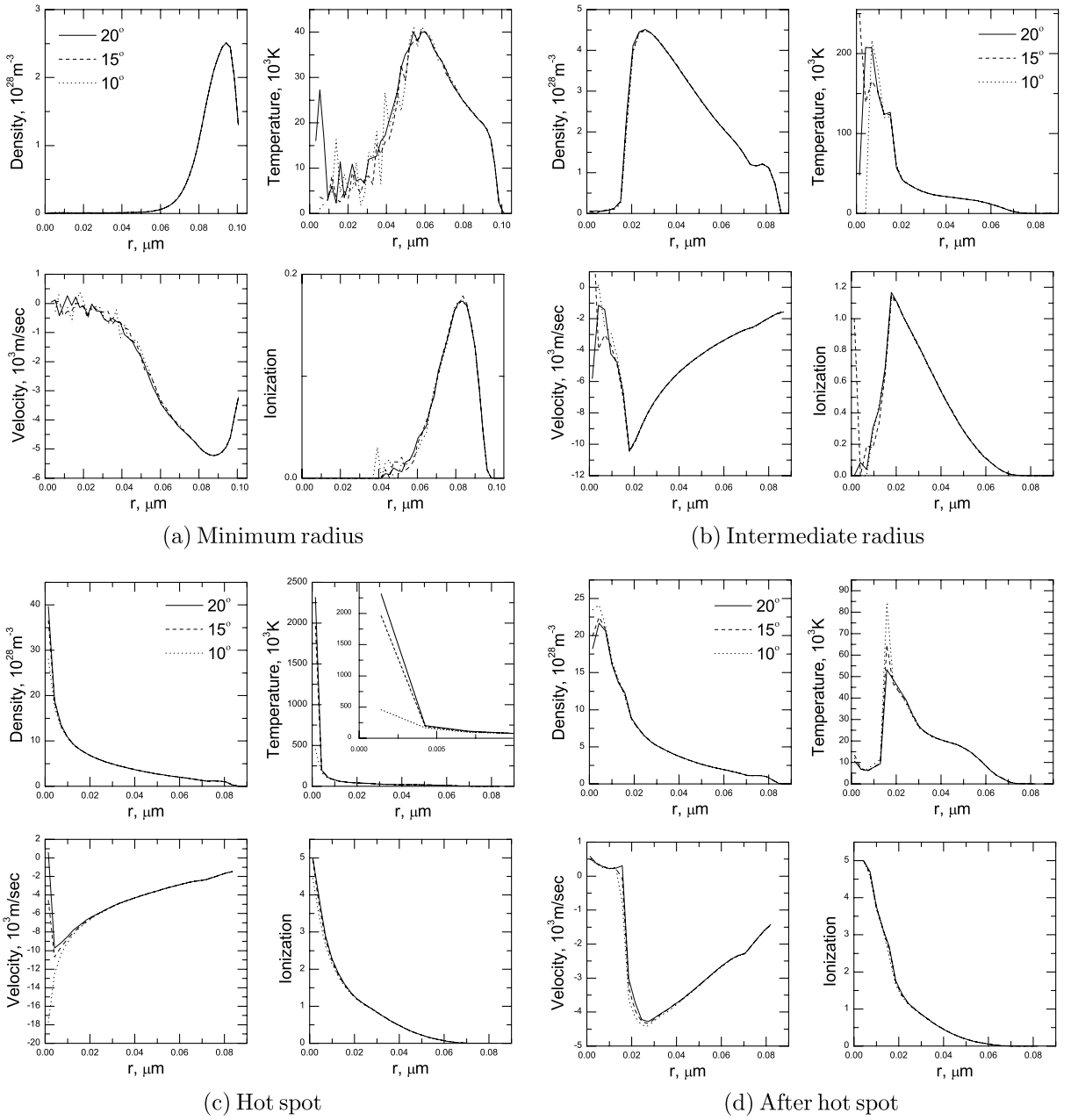

Fig. 3. The evolution of a Xenon bubble with the ambient radius of 0.79 μm and containing 50,000,000 atoms. 'Minimum radius' refers to the the minimum radius as predicted by the Rayleigh–Plesset equation. In the actual simulation, vacuum forms near the boundary and the bubble essentially continues its collapse past the predicted radius.

3.3. How small a cone is too small?

The above analysis may seem to indicate that cone simulations with an angle of 10° or more can be trusted while 5° cones give a significant error. There are, however, some additional criteria which come into play when selecting a cone angle. For example, the results we have presented depend on our (arbitrary) choice to average over (1/50)th of the total radius. Had we chosen to average over a smaller region, we would have likely had to choose larger cone angles to get adequate convergence. Conversely, if we settled for lower resolution, or per-

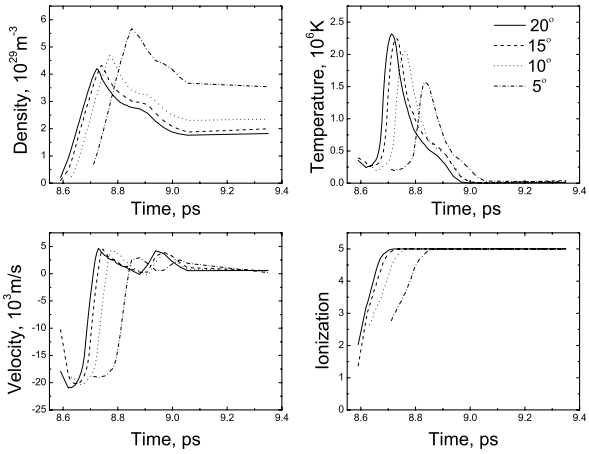

Fig. 4. The evolution of the center of the 50,000,000 atom Xenon bubble. Time = 0 corresponds to the minimum radius as predicted by the Rayleigh–Plesset equation. All data was obtained by averaging over a small core, (1/50)th of the total radius.

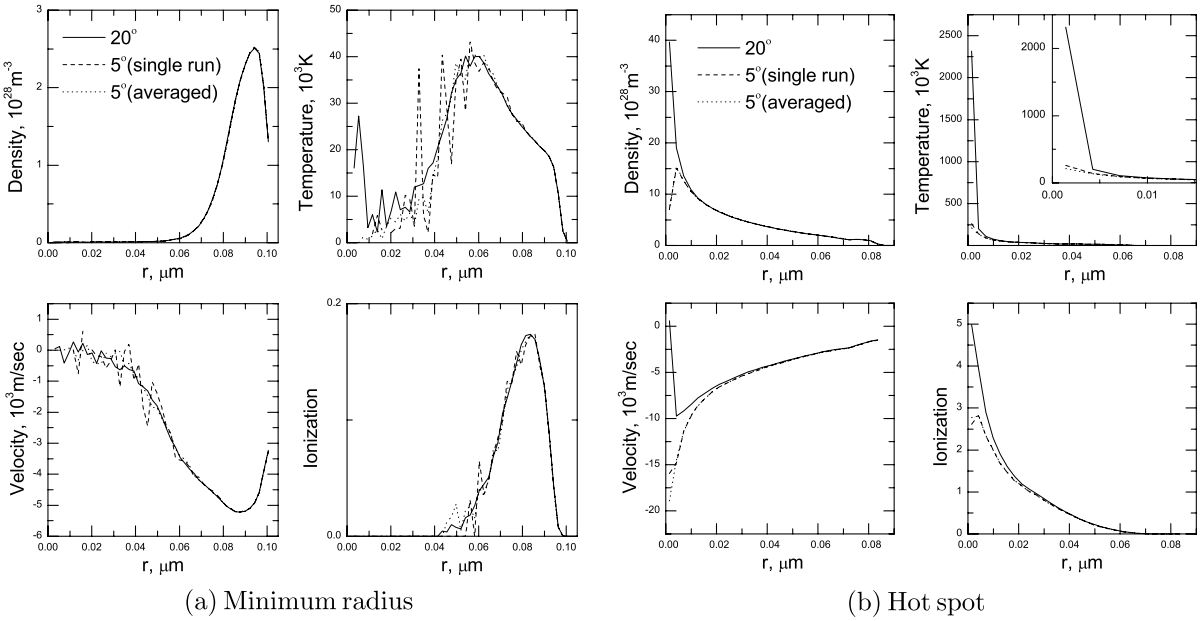

Fig. 5. Systematic vs. Statistical error. The jitter in the first figure is due to the statistically small number of atoms, and can be effectively eliminated by averaging over several runs. The second figure demonstrates systematic error introduced by the cone.

haps did not care that much about what was happening in the center of the bubble, smaller cone angles would suffice. Fig. 7 shows a snapshot of the system taken at some time between the minimum radius and the hot spot for 3°, 2° and 1° simulations and compares the results to simulations obtained with the much larger 20° cone. Though the smaller angles give some characteristic time shift (which at this stage is still unnoticeable with the 5° simulation), it is clear that these tiny cones give essentially the correct profiles for most of the bubble's volume.

Thus the optimum cone size clearly depends on what we care to know about the collapse. Many important questions, e.g. whether an imploding shock wave develops, do not require the knowledge of the processes occurring in the center. To answer such questions, small-angle cone simulations may be ideal, as they possess all the advantages of MD simulations, while at the same time being quite fast. For instance, small-angle cone simulations of Fig. 7 take just a few minutes to run on a modern PC.

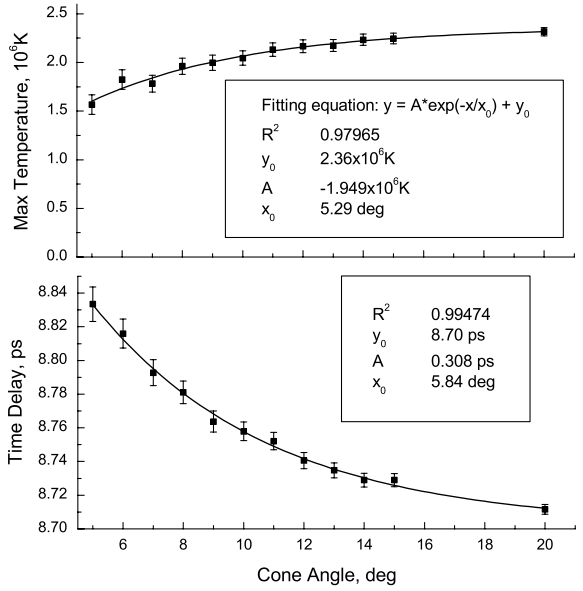

Fig. 6. Convergence study. The graphs show the dependence of the peak temperature and the time delay, defined as the time difference between the minimum radius and the peak temperatures, on the size of the cone. Both traces are fitted to the exponential decay function.

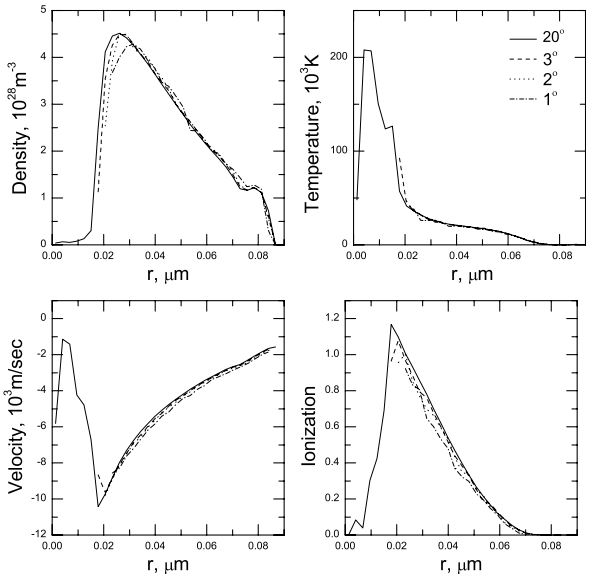

Fig. 7. Very small angles. The snapshot is taken at an intermediate radius, same as in Fig. 3(b). The graphs for small angles are missing points near the center due to a very low number of particles there.

4. Summary and future work

The one-dimensional nature of spherically symmetric macroscopic motion can be used to speed up MD calculations through the use of the cone geometry. Imploding shocks predicted in Refs. [7,21] can be captured with cones as small as 2°. Such simulations run in just a few minutes on a modern PC, which compares very favorably with the months required to run the complete system without symmetry reduction. These fast calculations are also capable of capturing a non-hydrodynamical aspect of the motion: namely that during the pre-focusing moments of shock wave motion the temperature spike precedes the density spike (e.g. Fig. 7).

This is due to the tail of the statistical distribution running ahead of the density signal. This behavior occurs in the same region as where the temperature varies significantly over distances shorter than a mean free path [11]. We refer to the steeply sloped density discontinuities as a shock wave because the simulations show that they move much faster (8000 m/s) than the sound velocity in the ambient gas at the leading edge. Indeed the shock moves faster than the sound velocity calculated for the peak of the temperature in the bubble.

In conclusion we would like to list a number of possible directions for improvement in our current model, some of which are necessary before attempting a comparison to experimental measurements.

- An immediate improvement would be to include the effects of dissipation into the Rayleigh–Plesset equation. This will slow the collapse and decrease temperatures. Note that, even then, shock waves appear in our (preliminary) simulations.
- The next step should be to couple self-consistently the Rayleigh–Plesset equation to the MD system. This means that the adiabatic pressure of Eq. (3) must be replaced with the actual pressure of the MD system measured at the boundary. Since the bubble is highly non-uniform during the later stages of the collapse, with the density being maximum near the boundary, this will further slow the motion of the wall.
- As mentioned in The model section, the Rayleigh–Plesset equation is derived for small Mach number motion and thus is invalid as a fundamental theory for SL. So, on the next level, it must be replaced with the Navier–Stokes equations for the surrounding fluid coupled to the MD system inside the bubble.
- In the final stages of the collapse the interatomic collisions become so frequent that the soft sphere model, otherwise prohibitively expensive computationally, may surpass the hard sphere model in computational efficiency. It is also physically appropriate to describe the high density regime with the real interaction potential.
- The assumption that the kinetic energy after an ionization event is equally distributed between electron, and ion and atom should be compared and perhaps replaced with the assumption that the electron's kinetic energy is negligible during the time scales under consideration [22]. This modification will raise temperatures.

Acknowledgments

We thank Paul Roberts, C.C. Wu, Brian Kappus and Emil Kirilov for valuable discussions. Research supported in part by DARPA. The research of the last author was also supported by NSERC Canada.

References

[1] B.P. Barber, R.A. Hiller, R. Lofstedt, S.J. Putterman, K.R. Weninger, Defining the unknowns of sonoluminescence, Phys. Rep. 281 (March) (1997) 65–143, 79).
[2] S.J. Putterman, K.R. Weninger, Sonoluminescence: how bubbles turn sound into light, Ann. Rev. Fluid Mech. 32 (1) (2000) 445–476.
[3] M.P. Brenner, S. Hilgenfeldt, D. Lohse, Single-bubble sonoluminescence, Rev. Mod. Phys. 74 (2) (2002) 425–484.
[4] D.F. Gaitan, L.A. Crum, C.C. Church, R.A. Roy, Sonoluminescence and bubble dynamics for a single, stable, cavitation bubble, The J. Acoust. Soc. Am. 91 (6) (1992) 3166–3183.
[5] D.J. Flannigan, K.S. Suslick, Plasma formation and temperature measurement during single-bubble cavitation, Nature 434 (2005) 52–55.
[6] C.C. Wu, P.H. Roberts, A model of sonoluminescence, Proc. R. Soc. A 445 (1994) 323–349.
[7] C.C. Wu, P.H. Roberts, Shock-wave propagation in a sonoluminescing gas bubble, Phys. Rev. Lett. 70 (22) (1993) 3424–3427.
[8] V.Q. Vuong, A.J. Szeri, D.A. Young, Shock formation within sonoluminescence bubbles, Phys. Fluids 11 (1) (1999) 10–17.
[9] W.C. Moss, D.B. Clarke, D.A. Young, Calculated pulse widths and spectra of a single sonoluminescing bubble, Science 276 (5317) (1997) 1398–1401.
[10] K. Yasui, Alternative model of single-bubble sonoluminescence, Phys. Rev. E 56 (6) (1997) 6750–6760.
[11] S.J. Ruuth, S. Putterman, B. Merriman, Molecular dynamics simulation of the response of a gas to a spherical piston: implications for sonoluminescence, Phys. Rev. E 66 (3) (2002) 036310.
[12] D.C. Rapaport, The Art of Molecular Dynamics Simulation, Cambridge University Press, Cambridge, England, 1998.
[13] R.A. Sadus, Molecular Simulation of Fluids: Theory, Algorithms and Object-orientation, Elsevier Science B.V., Amsterdam, 1999.
[14] K.Y. Kim, H.-Y. Kwak, J.H. Kim, Molecular dynamics simulation of collapsing phase for a sonoluminescing gas bubble in sulfuric acid solutions: a comparative study with theoretical results (atomic and molecular physics), J. Phys. Soc. Jpn. 76 (2) (2007) 024301-1–024301-11.

[15] P. Gaspard, J. Lutsko, Imploding shock wave in a fluid of hard-core particles, Phys. Rev. E (Statist. Nonlinear Soft Matter Phys.) 70 (2) (2004) 026306.
[16] B. Metten, W. Lauterborn, Molecular Dynamics Approach to Single-Bubble Sonoluminescence, vol. 524, AIP, 2000, pp. 429–432.
[17] C. Camara, S. Putterman, E. Kirilov, Sonoluminescence from a single bubble driven at 1 megahertz, Phys. Rev. Lett. 92 (12) (2004) 124301.
[18] G.A. Bird, Molecular Gas Dynamics and the Direct Simulation of Gas Flows, Oxford University Press, New York, 1998.
[19] K. Koura, H. Matsumoto, Variable soft sphere molecular model for inverse-power-law or Lennard-Jones potential, Phys. Fluids A: Fluid Dyn. 3 (10) (1991) 2459–2465.
[20] K. Koura, H. Matsumoto, Variable soft sphere molecular model for air species, Phys. Fluids A: Fluid Dyn. 4 (5) (1992) 1083–1085.
[21] H.P. Greenspan, A. Nadim, On sonoluminescence of an oscillating gas bubble, Phys. Fluids A: Fluid Dyn. 5 (4) (1993) 1065–1067.
[22] B. Kappus, private communication.